Numerical Simulation of the Hysteresis Phenomenon and Asymmetrical Configuration of Turbulent Gas Flow in an Over-Expanded Nozzle Flows

BENDERRADJI RAZIK[1,3], GOUIDMI HAMZA[2,3]
[1]Physics Department,
University of M'Sila- University Pole,
Road Bourdj Bou Arreiridj, M'sila 28000
ALGERIA

[2]Mechanics Department,
M[ed] El-Bachir El-Ibrahimi University,
Bordj Bou Arréridj,
ALGERIA

[3]Laboratory of Renewable Energies and Sustainable Development (LERDD),
Frères Mentouri University,
Constantine1-Algeria,
ALGERIA

Abstract: - The turbulent flow within Over-Expanded Nozzles is characterized by shock waves inducing unsteady separation of the boundary layer, which can exhibit both free and restricted detachment. This study investigates various physical phenomena encountered during the expansion regime, including supersonic jet formation, jet separation, adverse pressure gradients, shockwave interactions, turbulent boundary layers, compressible mixture layers, and large-scale turbulence. These complex phenomena significantly influence nozzle performance. Utilizing numerical simulations based on the resolution of Navier-Stokes equations via finite volume methods and employing the CFD-FASTRAN code, this research analyzes detachment characteristics, transition phenomena, and the predictive accuracy of different turbulence models. A test case from the ATAC project CNES-ONERA (Aerodynamics of Hoses and Back-bodies), is examined to elucidate the hysteresis phenomenon and asymmetrical configurations resulting from boundary layer detachment.

Key-Words: - nozzle, over-expanded, detachment, shockwave, unsteadiness, hysteresis phenomenon.

Received: January 17, 2024. Revised: August 3, 2024. Accepted: September 11, 2024. Published: October 29, 2024.

1 Introduction

The field of aerodynamics plays a crucial role in determining the technical specifications of launchers, facilitating performance calculations, and mitigating the impact of unsteady loads that can jeopardize the structural integrity of propulsion systems and harm payloads. Significant research has been devoted to the internal aerodynamics of propulsive nozzles, particularly focusing on their geometric evolution from the throat onwards. By abruptly expanding the section ratio, these nozzles enhance theoretical propulsion, particularly effective during flight phases at high altitudes where external pressures are minimal. Consequently, propellant gases undergo substantial expansion. However, during engine ignition on the ground, takeoff, and early flight phases, the nozzle encounters external pressures exceeding those at the outlet section, necessitating rapid adjustment of the propulsive flow pressure. This adaptation is achieved through a recompression shock positioned within the nozzle, known as the over-expansion shock. In instances of significant over-expansion, this shock induces turbulent boundary layer separation, characterized by its asymmetrical and unsteady nature, which generates lateral loads on the nozzle's structure.

In addition, internal shocks resulting from the Mach line focusing at the nozzle's throat have been observed in such configurations. These shocks create specific shock structures, triggering boundary layer separation and reattachment phases

characterized by intense fluctuations as the system transitions between different configurations. Despite some studies exploring the influence of internal shocks, the fundamental mechanisms underlying turbulent boundary layer reattachment remain poorly understood. This phenomenon is a primary driver of boundary layer reattachment and associated transients, warranting thorough investigation and analysis.

Flow analyses in supersonic convergent-divergent nozzles have been conducted, exploring various cross-sectional shapes and their effects on flow characteristics using ANSYS FLUENT 12.0, [1]. Important differences in temperature, pressure, and velocity between various nozzle configurations have been highlighted, emphasizing the influence of nozzle geometry on fluid flow characteristics. To conduct simulation assessments on convergent-divergent nozzles, outcomes of numerical modeling have been compared with data obtained from measurements using various turbulence models, including the K-ε and K-ω models, [2]. Differences observed have been attributed to wall friction, slip factor, and material characteristics, underscoring the necessity of carefully interpreting simulation results.

Reynolds-Averaged Navier Stokes simulations have been used to explore the influence of nozzle geometry on turbulence and flow characteristics, emphasizing the importance of mesh topology for result accuracy, [3]. Various nozzle shapes, flow characteristics, and shock effects on divergent nozzle parts have been investigated, shedding light on performance factors under different conditions, [4], [5], [6].

Furthermore, the phenomenon of unsteady and asymmetric detachment in conical or curved nozzles has been emphasized. Experiments have revealed a transition from symmetrical to asymmetrical flow regimes, with distinct pressure ratio ranges defining different flow types, relatively unaffected by the nozzle's divergent angle, [7].

Overall, these studies highlight the intricate interplay between nozzle geometry, flow dynamics, and shock interactions, highlighting the need for comprehensive numerical simulations and experimental investigations to deepen our understanding of nozzle flow phenomena.

2 Numerical Procedure

2.1 Optimization of the Numerical Simulation

The study was conducted on a test case of the ATAC project. The simulated nozzle is a 2D divergent converging nozzle; Figure 1 with a section ratio of 1.7, a Mach number at the output is greater than 2, and a divergence half-angle of 10 °.

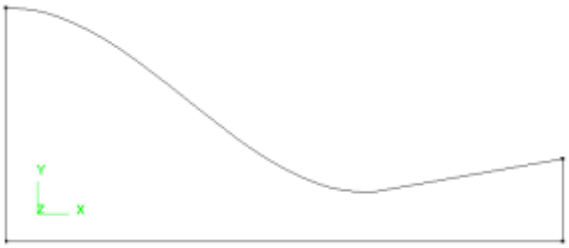

Fig. 1: The nozzle profiles employed in the 2D calculations

2.2 CFD Code Description

The numerical study has been conducted using a finite volume Reynolds-Averaged-Navier-Stokes (RANS) solver (CFD-FASTRAN) developed by the CFD Research Corporation. This code offers two upwind differencing schemes with a variety of higher-order limiters to calculate the convective terms in the transport equations. Both explicit and fully implicit time integration schemes are available for steady and unsteady flow simulations.

The code is based on a cell-centered finite volume discretization. Inviscid fluxes may be computed using Roe's flux difference splitting scheme and Van Leer's flux vector splitting. Both schemes are first order spatially accurate. Flux limiters may however be used to raise spatial accuracy. For the Min-mod and Van Leer limiter, the accuracy is 2nd order while for Osher Chakravarty limiter the accuracy is up to third order. CFD-FASTRAN has five turbulence models (k-ε, k−ω, k−ω SST Menter, Spalart-Allmaras and Baldwin-Lomax). For this study, the flux vectors are evaluated, at each time step, using Roe's upwind flux difference splitting, with a MINMOD flux limiter in order to achieve a high-order spatial accuracy. Three turbulence models are used: Baldwin-Lomax, Spalart-Allmaras, and k – ω SST. Time integration is achieved using a fully implicit scheme. Local time stepping is also used to accelerate convergence to a steady state.

2.3 Boundary Conditions and Meshing

Figure 1 depicts the profile of the nozzle used in the 2D calculations, highlighting the geometric features required for the computational study. The mesh used in the simulations is made up of four separate blocks, each suited for computations corresponding to the whole nozzle shape. In addition to Figure 1, Figure 2(a) and Figure 2(b) show visual representations of the meshes used in the numerical

calculations, together with their associated boundary conditions.

The meshing approach used in this study includes numerous zones to properly capture flow dynamics. The primary zone, located within the nozzle, has a high concentration of cells, allowing for fine resolution of flow physics. Zone (2) also covers the external area downstream of the nozzle, whereas Zones (3) and (4) are strategically located at the nozzle's upper and lower borders, respectively. This hierarchical meshing method allows for more accurate and efficient simulations by taking into account the unique flow characteristics of each zone.

Mesh refinement near the walls enhances the accuracy of boundary simulations. Numerical computations consider both turbulent and stationary flow conditions. At the inlet of the nozzle, a subsonic input condition is enforced, specifying generating conditions and velocity direction. The nozzle walls and upstream outer domains exhibit adhesion and adiabatic properties. Non-reflective conditions are applied to the upper and lower boundaries. Finally, a subsonic output condition is imposed on the downstream boundary, necessitating significant longitudinal extension to facilitate the formation of a subsonic jet through momentum diffusion induced by viscosity.

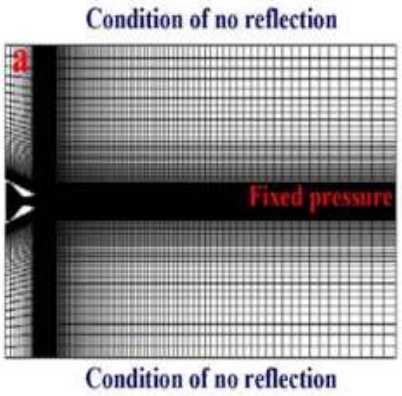

(a)

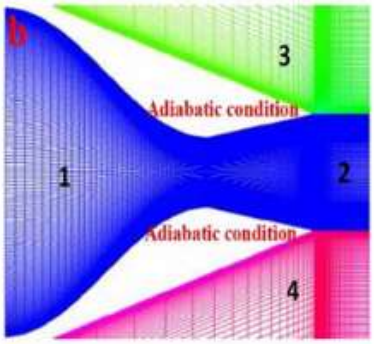

(b)

Fig. 2: The structured mesh of the nozzle used in the numerical simulations

2.4 Influence of Turbulence Models

In numerical calculations, the choice of the turbulence model significantly affects the results. Several models were tested: the algebraic model of Baldwin_Lomax, the model with an equation of Spalart_Allmaras and the models with two equations of transport (k-ε and k-ω).

Figure 3 shows the influence of turbulence models on the distribution of wall pressure along the nozzle divergence. Numerical calculations are carried out at NPR = 6. We note that all the models used, for example, the case of the model k-ε. The model of Spalart Allmaras, Balwin_Lomax and k-ω reproduce the area of separation appropriately compared to the experiment. Given these results, the k-ω model will be used in subsequent 2D calculations.

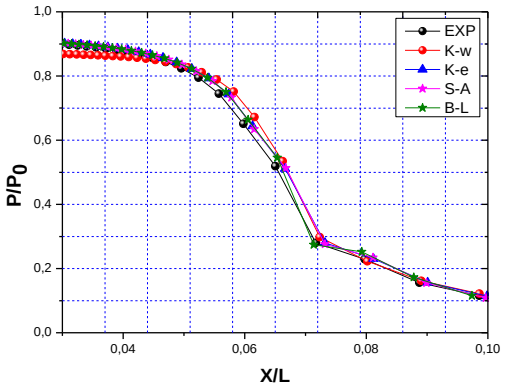

Fig. 3: The impact of turbulence models on pressure distribution at NPR = 6

3 Validation of the Results

Figure 4 presents the Mach number iso-contours, demonstrating the validation of our calculations against experimental data [1] and numerical results [8]. Remarkably, the three configurations exhibit close resemblance, indicating excellent agreement. Shock-like or relaxation wave structures are evident in the downstream flow, with numerical observations closely matching experimental findings.

Figure 5 compares the upper wall pressure distribution between experimental and numerical simulations for the overpressure regime at NPR = 3.80. The results demonstrate a high level of agreement between calculation results and experimental data. Both distributions exhibit similar trends, although a slight disparity is observed in the pressure plateau after the separation point.

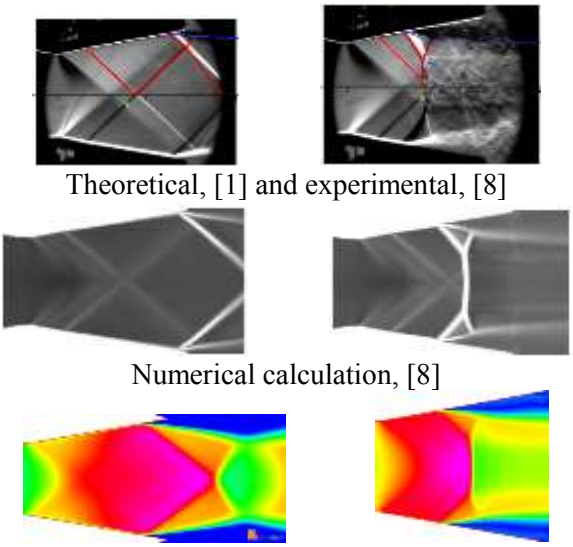

Fig. 4: Comparison of experimental and theoretical configurations

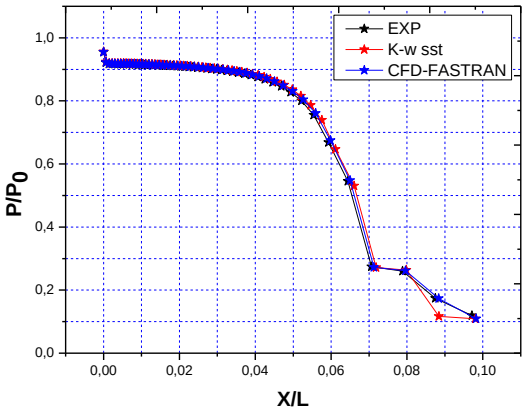

Fig. 5: Distribution of upper wall parietal pressure at NPR = 3,80. Comparison of our findings with [2]

4 Results and Discussion

4.1 Hysteresis Phenomenon and Asymmetric Flow Configuration

To replicate the hysteresis phenomenon in the supersonic nozzle, we utilize the NPR expansion rate, defined as the ratio between the nozzle generating pressure and the ambient pressure (Pi0 / Pa). This ratio plays a pivotal role in parameterizing the calculations, as it is responsible for the formation of a recompression shock. However, the presence of this shock can penetrate into the nozzle, leading to the delamination of the boundary layer. Depending on the scenario, the boundary layer may either detach without reattachment (Free Shock Separation - FSS), or it may detach and subsequently reattach downstream, forming a recirculation bulb (Restored Shock Separation - RSS). The unsteadiness of this interaction generates significant oscillating mechanical loads and intense variations in heat flux on the nozzle wall. This phenomenon, initially demonstrated experimentally, was subsequently confirmed numerically by [8].

Numerical simulations were conducted using 2D Reynolds-Averaged Navier-Stokes (RANS) calculations across various NPRs, ranging from NPR = 1.8 to NPR = 5.42. The objective was to observe different configurations, including asymmetric and symmetrical detachment, as well as the manifestation of the hysteresis phenomenon. Figure 6 depicts that beyond a critical NPR, the flow within the nozzle becomes asymmetric relative to the nozzle axis, corroborating experimental findings. This asymmetric configuration has been observed in other geometries as well, as documented by [9], [10] and [11].

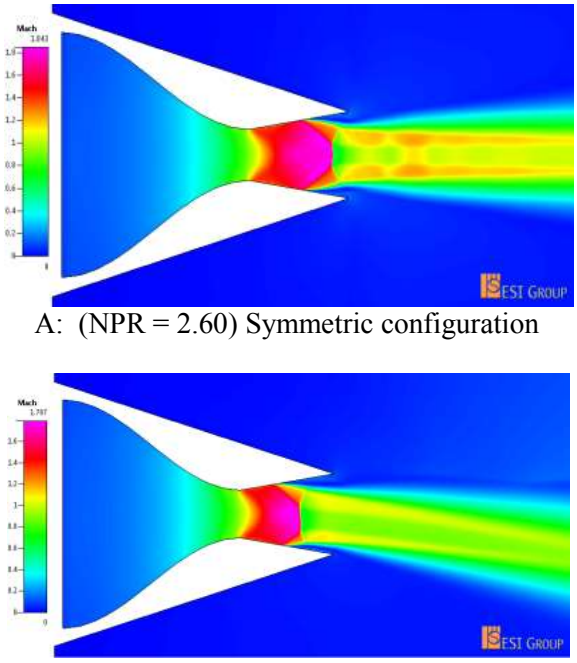

A: (NPR = 2.60) Symmetric configuration

B: (NPR = 2.15) Asymmetric configuration

Fig. 6: Visual representation of numerical flow configurations at two different NPRs

To explore whether the critical NPR is consistent for both increasing and decreasing NPR values, simulations were initiated at NPR = 5.42 and progressively decreased to NPR = 1.8. At each step, convergence was achieved for a steady stationary solution, starting from the converged initial field of the preceding NPR. The multi-stage numerical simulation results are illustrated in Figure 7.

Initially, the flow exhibits symmetry. However, at NPR = 1.90 (critical NPR), asymmetry emerges and persists as the NPR further decreases.

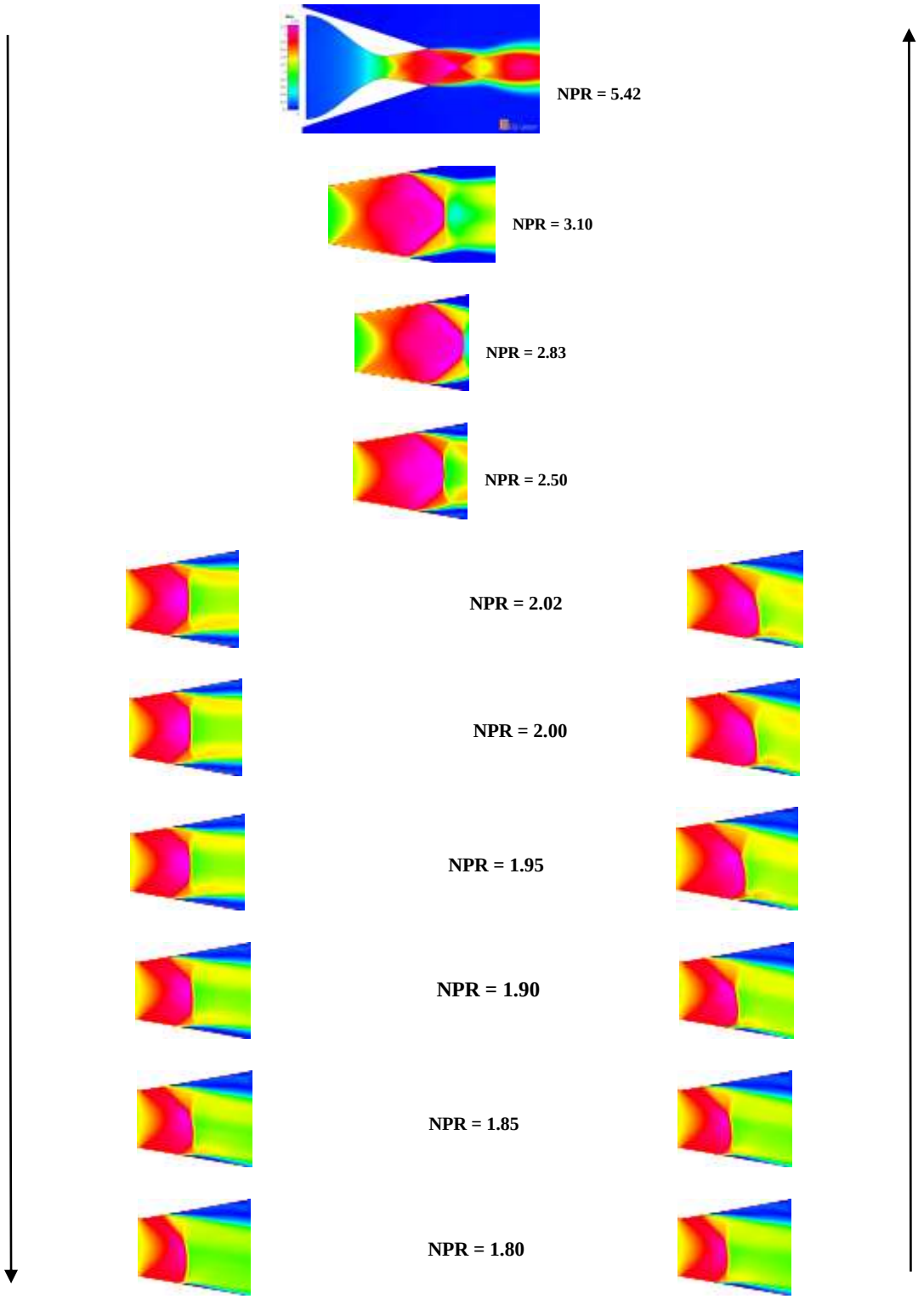

Fig. 7: Hysteresis phenomenon resulting from variations in the NPRs expansion ratio

Consequently, the relaxation ratio gradually increases. Notably, the flow abruptly transitions to symmetry, yet asymmetry persists when the NPR exceeds the critical NPR (during the increasing NPR case). This suggests that if the flow is initialized with an asymmetric configuration, achieving symmetry requires a significantly higher NPR, with the critical NPR slightly differing from that obtained in the increasing NPR case. Conversely, as the NPR decreases, asymmetry begins to manifest, with the symmetrical configuration ceasing to exist below this threshold (as observed at NPR = 1.90). Upon increasing the NPR value again, such as at NPR = 2.50, the flow regains symmetry with respect to the nozzle's axis of symmetry, maintaining symmetry beyond this value. The existence of a double zone of NPR, where both configurations are possible, signifies the presence of the hysteresis phenomenon. Additionally, for significant relaxation rates such as NPR = 5.42 and NPR = 3.80, a regular reflection of the relaxation shock occurs. Lowering the relaxation rate results in Mach reflection, accompanied by a rise in the detachment point. In all these cases, the separation is free, and the interaction between the internally reflected shock and the relaxation shock is evident. At NPR = 2.02, the incident internal shock intersects the Mach disk, consistent with experimental observations.

The separation point is similarly located far upstream. Additionally, a free detachment of the boundary layer induces deformation of the Mach disk towards the lower wall, where reattachment occurs. This tendency is reflected in the shape of the pressure curves, which exhibit a point of inflection on the lower wall corresponding to the recirculation bubble.

Calculations at lower NPRs of 1.8 yield consistent results. However, the results for low expansion rates are not presented. In conclusion, the study underscores the significant dependence of flow symmetry on NPR variation in the nozzle, which holds substantial industrial relevance concerning the structural integrity of nozzles during rocket and/or spaceship launches.

The previous observations can be depicted in Figure 8, where the existence of a double NPR zone where both configurations are possible is highlighted. The hysteresis phenomenon, induced by the variation in NPR pressure ratio, is clearly reproduced by the numerical calculation, as illustrated by the density gradient contours in Figure 7. Indeed, for a given pressure ratio, one observes, depending on the direction of passage, either a symmetrical configuration or an asymmetrical configuration. This phenomenon is characterized by a decrease, followed by an increase in the NPR pressure ratio, defined by the combination of the two transition passages, from Sym→Asym and Asym→Sym. Regarding the NPR effect calculation: The NPRcrit-asymest transition is obtained for a decreasing pressure ratio of 1.90. The NPRcrit-symest transition is obtained for an increasing pressure ratio of 2.50.

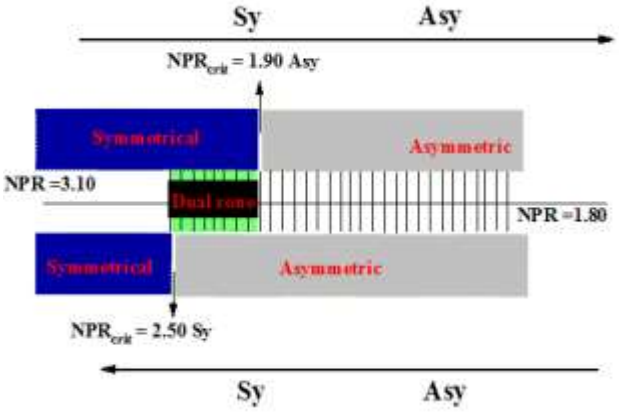

Fig. 8: Diagram of the Sym↔Asym hysteresis phenomenon obtained through 2D simulations induced by the NPR effect

4.2 Influence of Flow on Pressure Relationships

Figure 9(a) portrays the upper parietal pressure ratios, corresponding to the scenario where the relaxation number increases, while Figure 9(b) illustrates the lower parietal pressure ratios for the scenario where the expansion number decreases. These figures highlight a notable difference in the position of the separation point, particularly pronounced for NPR values below 3.80. However, as the relaxation rate decreases, this distinction diminishes, and the detachment occurs further downstream in the numerical simulations.

The numerical simulations effectively capture key features such as the pressure plateau following detachment and the pressure jump induced by the internal shock. Several factors contribute to deviations observed in pressure ratios and the position of the separation point in the 2D numerical calculations:

- The selection or parameterization of the turbulence model.
- Refinement of the near-wall mesh.
- Accurate estimation of the displacement thickness of the boundary layer developing on both walls of the nozzle.

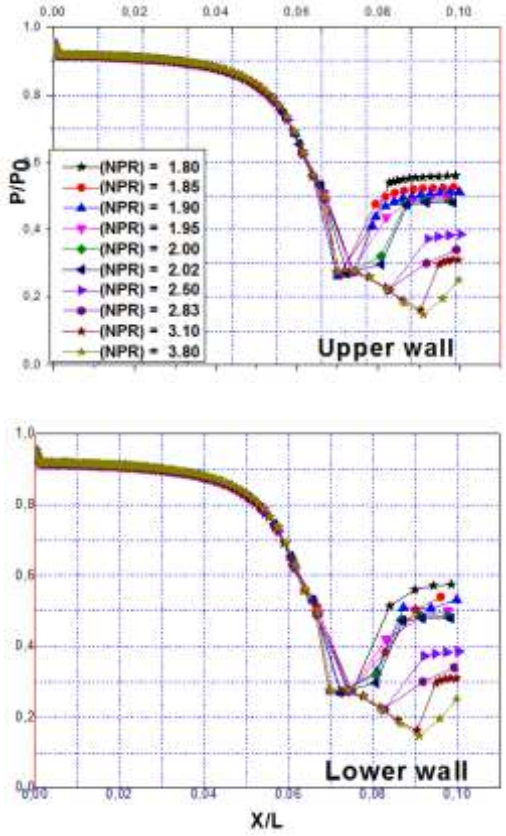

Fig. 9(a): Comparison of pressure ratios (NPR increasing)

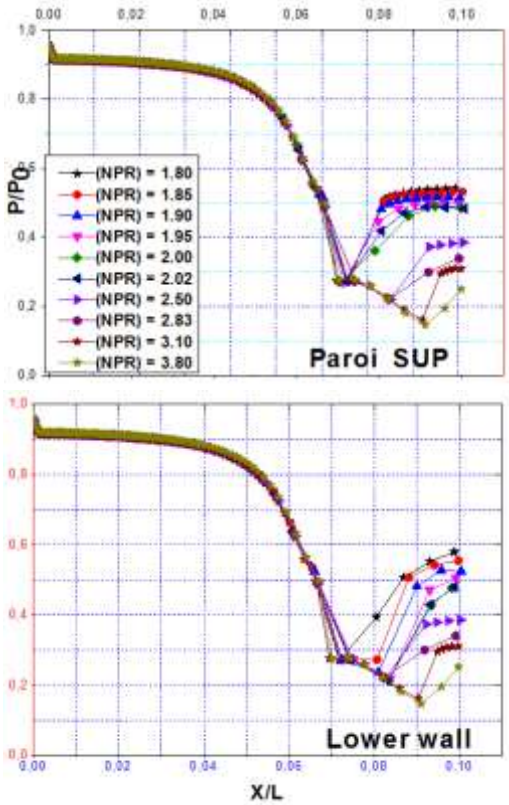

Fig. 9(b): Comparison of pressure ratios (NPR decreasing)

5 Conclusion

The hysteresis phenomenon associated with the interaction between shock waves and boundary layers is a significant concern across various fields of aeronautics. This interaction occurs in both internal aerodynamics, such as air intakes and scramjets, and external aerodynamics, including transonic flow with extrados shocks and Over-Expanded Nozzle flows. Its presence poses practical challenges as it induces intense unsteady stresses, which can cause structural fatigue and eventual failure. Additionally, it can lead to operational instabilities in engines, such as compressor surges and combustion instability in scramjets.

Declaration of Generative AI and AI-assisted Technologies in the Writing Process

During the preparation of this work the authors used ChatGPT / QuillBoT in order to check grammar, spelling, references and rephrase some sentences.. After using this Grammar Checker and Paraphrasing Tool, the authors reviewed and edited the content as needed and take full responsibility for the content of the publication.

References:

[1] Girard, S. Study of Shock Interferences in Overexpanded Nozzles with Internal Shock (Etude des Interférences de Choc dans les tuyères surdétendues à choc interne), Doctoral dissertation, Paris 6, 2009, [Online]. https://theses.fr/2009PA066439 (Accessed Date: March 21, 2023).

[2] Satyanarayana, G., Varun, C., & Naidu, S. S. CFD analysis of convergent-divergent nozzle. *Acta Technica Corviniensis-Bulletin of Engineering*, Tomo 6, N.º 3, (2013): 139-144, [Online]. https://www.proquest.com/openview/a4eafbc0b2b81def12e0dbd72ec7c96a/1?pq-origsite=gscholar&cbl=616471 (Accessed Date: September 12, 2022).

[3] Shariatzadeh, O. J., Abrishamkar, A., & Jafari, A. J. Computational Modeling of a Typical Supersonic Converging-Diverging Nozzle and Validation by Real Measured Data. *Journal of Clean Energy Technologies*, Vol. 3(3), 2015, 220–225. https://doi.org/10.7763/jocet.2015.v3.198.

[4] Yu, Y., Shademan, M., Barron, R. M., & Balachandar, R. CFD Study of Effects of Geometry Variations on Flow in a Nozzle. *Engineering Applications of Computational*

Fluid Mechanics, Vol. 6(3), 2012, 412–425. https://doi.org/10.1080/19942060.2012.11015432.

[5] Hussain, A. K. M. F., and Ramjee, V. "Effects of the Axisymmetric Contraction Shape on Incompressible Turbulent Flow." ASME. *J. Fluids Eng*. March, Vol. 98(1), 1976, 58–68. https://doi.org/10.1115/1.3448210.

[6] Pandey, K. M., & Singh, A. P. CFD Analysis of Conical Nozzle for Mach 3 at Various Angles of Divergence with Fluent Software. *International Journal of Chemical Engineering and Applications*, Vol. 1 (2), 2010, 179–185. https://doi.org/10.7763/ijcea.2010.v1.31.

[7] Pansari, K., & Jilani, S. A. K. Numerical investigation of the performance of convergent divergent nozzle. *International Journal of Modern Engineering Research*, Vol. 3(5), 2013, 2662-2666, [Online]. http://www.ijmer.com/papers/Vol3_Issue5/AJ3526622666.pdf (Accessed Date: May 7, 2023).

[8] Sellam, M., Fournier, G., Chpoun, A., & Reijasse, P. Numerical investigation of overexpanded nozzle flows: Asymmetrical configuration and hysteresis phenomenon. *Shock Waves*, Vol. 24(1), 2014, 33-39. DOI: 10.1007/s00193-013-0458-3.

[9] Lawrence, R. A. Symmetrical and unsymmetrical flow separation in supersonic nozzles. Southern Methodist University, ProQuest Dissertations & Theses, 1967. 6809667, [Online]. https://www.proquest.com/openview/578fe23b549dcfaaf418191f2fed9cdc/1?pqorigsite=gscholar&cbl=18750&diss=y (Accessed Date: September 21, 2022).

[10] Bourgoing, A., & Reijasse, P. Experimental analysis of unsteady separated flows in a supersonic planar nozzle. *Shock Waves*, Vol.14, 2005, 251-258. DOI: 10.1007/s00193-005-0269-2.

[11] Reijasse, P., Corbel, B., & Soulevant, D. Unsteadiness and asymmetry of shock-induced separation in a planar two-dimensional nozzle-a flow description. In 30th Fluid Dynamics Conference. 1999 (p. 3694) Norfolk,VA,U.S.A. https://doi.org/10.2514/6.1999-3694.

Contribution of Individual Authors to the Creation of a Scientific Article

The authors equally contributed in the present research, at all stages from the formulation of the problem to the final findings and solution.

Sources of Funding for Research Presented in a Scientific Article or Scientific Article Itself

No funding was received for conducting this study.

Conflict of Interest

The authors have no conflicts of interest to declare that are relevant to the content of this article.